

4 Importance of Initial and Boundary Conditions for Ozone Modeling in Very Complex Terrains

Submitted as Jiménez, P., Parra, R., Baldasano, J.M., 2005. Influence of initial and boundary conditions for ozone modeling in very complex terrains: a case study in the northeastern Iberian Peninsula. Journal of Geophysical Research.

4.1 Introduction

A three-dimensional air quality model contains a set of stiff differential equations, which describes the time evolution of chemical species in the atmosphere. Initial and boundary conditions are required in order to solve these equations. The initial conditions are specified within the simulation domain at the beginning of the simulation, while boundary conditions are prescribed throughout the simulation period. Ideally, initial and boundary conditions should be determined based on observations. However, such high-resolution observations are generally not available. Model studies of photochemical pollutants pertained to a limited region and over a limited time period to some degree will be affected by the assumed initial and boundary conditions. The extent of influence will be most profound shortly after the model simulation has been initialized and close to the model boundaries. However, the impact of these conditions could depend on several factors: quenching, depositions, chemical reactions, etc.

Since initial and boundary conditions are usually specified in some extent of presumption, it is important to minimize the influence of initial and boundary conditions in the model calculations. Three general methods are used to specify the initial and boundary conditions (National Research Council, 1991): (1) use the output of a larger domain simulation; (2) use the objective or interpolated techniques when applying ambient observed data; and (3) isolate simulation domain from significant sources.

Liu *et al.* (2001) quantified the influences of initial and boundary conditions through theoretical analysis of the governing equation and verified the results by applying the SARMAP air quality model. The influence of boundary conditions decreases during the downwind transport, and is significant to a selected site when the arrival time of boundary condition is short and the species lifetime is long. Therefore, influences of boundary conditions are more important for area near domain boundaries.

Berge *et al.* (2001) have indicated that the influence of initial conditions could be minimized through spin-up or start-up prior to formal simulations. The influences of initial conditions

basically depend on species lifetime. The impacts of initial conditions on a given site decrease with simulation time and significantly affect the species concentrations before the arrival of boundary conditions, and disappear after their arrival.

The species evolution in the downwind area is continuously affected by upwind boundary conditions through this spin-up process. Thus, Seinfeld and Pandis (1998) have suggested a few rules to reduce the influences of boundary conditions. First, include all the sources that may have potential effects on the given region in the simulation domain. Second, include the sources implicitly in boundary conditions; and third, apply the simulation results of a larger model domain to the boundary conditions of smaller simulation domains within. This last procedure leads to the utilization of multiscale simulations and is called multiscale-nested modeling, which allows capturing the non-linearities of atmospheric chemistry, yet conserving computational resources. Multiscale-nested models are considered the current state-of-the-science for air quality modeling (Russell and Dennis, 2000).

A description of the process of initialization and generation of boundary conditions for MM5-EMICAT2000-CMAQ through performing simulations in the entire Iberian Peninsula, and using a multiscale approach is shown in this Chapter. The wider domain is coupled via one-way nesting to the domain of the northeastern Iberian Peninsula, in order to provide the necessary boundaries. Furthermore, an analysis of the influences of initial and boundary conditions and their sensitivity is presented, indicating the necessity of a correct initialization of the model by means of spin-up or start-up procedures; and also the availability of good-quality boundary information when performing simulations in very complex terrains.

4.2 Multiscale-Nested Simulation Approach

Indications of the National Research Council (1991), Seinfeld and Pandis (1998) and Liu *et al.* (2001) were followed for the northeastern Iberian Peninsula, in order to minimize the impacts of initial and boundary conditions in the simulations and to maximize local characteristics. In this section, a short description of the methods used for the nested simulation is indicated.

4.2.1 Nesting Approach within MM5-EMICAT2000-CMAQ

Multiscale-nesting technique grids are needed to provide the required high-resolution simulations. At present, Models-3/CMAQ framework allows only static grid nesting (Byun *et al.*, 1999). In static grid nesting, finer grids are nested inside coarser grids. The resolution and the extent of each grid are determined *a priori* and remain fixed throughout the simulation. Static grid nesting conserves mass and preserves transport characteristics at the interfaces of grids with different resolutions (Odman *et al.*, 1995). It allows the effective interaction between different scales with an efficient use of computing resources.

Static nesting techniques allow one-way or two-way exchange of information among finer and coarser grids. The only difference between the one-way and two-way nesting is whether concentrations in coarser grid simulations are updated with the finer grid simulations through the feedback processors or not. Soriano *et al.* (2002) studied the influence of one-way and two-way nesting techniques over the very complex terrain of the northeastern Iberian Peninsula under a situation of low synoptic forcing. Differences in the simulated fields are significant when choosing one or another nesting technique, yielding the two-way simulation worst results when evaluating the model against ambient data. Therefore, the decision of considering one-way approaches was taken for the simulations performed here.

In one-way nesting, the primary concern is the mass conservation at the grid interface where boundary conditions are input to the finer grid using the coarser resolution. The advective flux at the inflow boundaries of the finer grid is the flux as determined by the coarser solution that passes through this interface (Byun *et al.*, 1999).

4.2.2 EMEP Emissions for the External Domain: Iberian Peninsula

Emissions used for the external domain of the Iberian Peninsula were derived from EMEP (www.emep.int) emissions database of year 2000, on an hourly basis and lumped according to Carbon Bond IV chemical mechanism (Gery *et al.*, 1989). Chemical species considered were nitrogen oxides, non-methane volatile organic compounds, sulfur dioxide, sulfates, carbon monoxide and ammonia. The annual value for total emissions of these categories was transformed in hourly emissions applying the factors suggested by Stein (2003) and Parra (2004). Those factors distinguish, for each area of EMEP inventory included in the domain, different ratios of emissions according to the month, the day of the week and the hour of day. Vertical distribution of emissions was implemented following the EMEP indications. Cells from the European EMEP mesh have a resolution of 50km in polar coordinates; but these emissions were interpolated into a grid of 24km resolution in Lambert coordinates, as needed by MM5-EMICAT2000-CMAQ.

Biogenic emissions (included in EMEP sector 11) were not derived from EMEP, but estimated following the methods implemented in EMICAT2000 (Parra *et al.*, 2004), that were previously referenced in Section 2, using the land-use map derived from NATLAN2000 and the United States Geological Survey according to the methodology by Pineda *et al.* (2004), and adapting the resulting land-uses to the 22 categories of EMICAT2000. Meteorological data (solar radiation and temperature) were derived from the simulations for Domain 1 performed with MM5 meteorological model. The emissions factors and the density of foliar biomass correspond to the results by Parra *et al.* (2004) for a typical environment in the Iberian Peninsula (Mediterranean, etc.).

The speciated hourly emissions are obtained from hourly emissions, applying the equation 4.1:

$$E_{eij} = \frac{E_{ei} \cdot F_{eij} \cdot RtT_e \cdot 10^6}{Pmol_i} \quad (4.1)$$

where:

E_{eij} : emission (mol h^{-1}) of the category j of the CBM-IV, produced by pollutant i (CO, NO_x , SO_x , NMVOCs) of the EMEP category e .

E_{ei} : emission (t h^{-1}) of the pollutant i (CO, NO_x , SO_x , NMVOCs) of the EMEP category e .

F_{eij} : transformation factor for the category j of the CBM-IV, that corresponds to the i pollutant of the EMEP category e .

RtT_e : factor of transformation of the emissions of EMEP category e , in order to include the methane to the emissions of NMVOCs. It responds to the "ROG to TOG" value indicated in the speciation profiles proposed by US EPA (US EPA, 2003). For CO, NO, NO_2 and SO_2 , SO_4 and NH_3 this factor has a value of 1.

$Pmol_i$: molecular weight of the i pollutant (g mol^{-1}). For NMVOCs, this value is 1.

Table 4.1 shows the values of F_{eij} and $Pmol_i$ that define the speciation profiles for the emissions of CO, NO_x and SO_x . Tables 4.2 and 4.3 depict the values of F_{eij} and RtT_e that define the speciation profiles selected for the emissions of NMVOCs.

Therefore, Figure 4.1 indicates the distribution of biogenic emissions of non-methane volatile organic compounds during 15 August, 2000, in Domain 1, in order to perform simulations for obtaining the initial and boundary conditions for the inner domain of the northeastern Iberian Peninsula. Figure 4.2 depicts the distribution of the emissions at 1200UTC of 13 August, 2000, for the species nitrogen monoxide and toluene, at surface and 150m in altitude

Table 4.1. Values of F_{eij} and $Pmol_i$ for the speciation of hourly emissions of CO, NO_x and SO_2 (adapted from Parra, 2004).

EMEP Category	F_{eij}				$Pmol_i$			
	CO	NO	NO_2	SO_2	CO	NO	NO_2	SO_2
1	1	0.62	0.05	1	28	30	46	64
2	1	0.62	0.05	1	28	30	46	64
3	1	0.62	0.05	1	28	30	46	64
4	1	0.5869	0.1	1	28	30	46	64
5	1	0.5869	0.1	1	28	30	46	64
6	Not Applicable							
7	1	0.62	0.05	1	28	30	46	64
8	1	0.62	0.05	1	28	30	46	64
9	1	0.62	0.05	1	28	30	46	64
10	1	0.5869	0.1	1	28	30	46	64
11	1	0.5869	0.1	1	28	30	46	64

Table 4.2. Values of RtT_e and F_{eij} and for the speciation of hourly emissions of NMVOCs for categories FORM, NR, PAR and TOL (adapted from Parra, 2004)*.

<i>EMEP Category</i>	<i>RtT_e</i>	<i>FORM</i>	<i>NR</i>	<i>PAR</i>	<i>TOL</i>
1	1.735	0.0083250085	0.02263695200	0.023933859	0.0001085305
2	1.735	0.0083250085	0.02263695200	0.023933859	0.0001085305
3	1.735	0.0083250085	0.02263695200	0.023933859	0.0001085305
4	1	0.0005246890	0.01291847300	0.026979413	0.0005925410
5	1.12	0	0.03011175600	0.036440673	0
6	1.03	0.0004895100	0.00451618200	0.027709807	0.0007216130
7	1	0.0002843100	0.00492621000	0.036115400	0.0016858100
8	1	0.0016836000	0.00362780000	0.045474900	0.0001894000
9	83.33	0	0.06104173359	0.001068438	0.0000108531
10	1	0.0005246890	0.01291847300	0.026979413	0.0005925410
11	1	0	0.5	8	0

*See legend in Table 4.3

Table 4.3. Values of F_{eij} and for the speciation of hourly emissions of NMVOCs for categories ALD2, ETH, OLE, XYL and ISOP (adapted from Parra, 2004).

<i>EMEP Category</i>	<i>ALD2</i>	<i>ETH</i>	<i>OLE</i>	<i>XYL</i>	<i>ISOP</i>
1	0	0	0	0	0
2	0	0	0	0	0
3	0	0	0	0	0
4	0.000763079	0.001289176	0.001898605	0.000398111	0.000058720
5	0	0	0	0	0
6	0.001688332	0.000566755	0.002569395	0.000624344	0.000215796
7	0.001125800	0.000868210	0.001779060	0.001444350	0
8	0.002979000	0.001539100	0.001668100	0.000282000	0
9	0	0	0.000007340	0.000009419	0
10	0.000763079	0.001289176	0.001898605	0.000398111	0.000058720
11	1.5	0	0.5	0	1

^{1,2,3}Responds to an average of speciation profiles 10100601 (electrical generation, natural gas) and 10100401 (electrical generation, residual oil) proposed by US EPA (US EPA, 2003).⁴Responds to profile 0 (applicable to industrial processes) (US EPA, 2003).⁵Profile 1011 (oil and gas production, crude oil production) (US EPA, 2003).⁶Profile 9028 (solvent utilization) (US EPA, 2003).⁷Profile deduced from on-road emissions (Parra, 2004; Parra and Baldasano, 2004).⁸Profile for emissions of diesel tourisms (Parra, 2004)⁹Profile 202 (waste disposal, treatment and recovery, landfills, municipal) (US EPA, 2003)¹⁰Profile 0 (applicable to agricultural production – livestock) (US EPA, 2003)¹¹Profile for biogenic emissions (Parra, 2004; Parra *et al.*, 2004)

4.3 Results and Discussions

Simulation was started at 0000UTC of 13 August, 2000, and extends for a period of 72 hours. A description of the meteorological conditions is found in Section 2.1. The wider domain (D1) covers an area of 1392 x 1104 km² centered in the Iberian Peninsula, with a horizontal resolution of 24-km and 16 vertical layers to cover the troposphere. Information related to the boundaries has been supplied from Domain 1 (D1) previously described, into an inner domain through a one-way nesting approach. Simulation of Domain 2 (D2) covers an inner area of 272 x 272 km² in the northeastern Iberian Peninsula. Model resolution for this second domain is 2-km horizontally, and 16 layers of variable thickness in altitude, as indicated in Chapter 2 of this document. Ozone

concentrations over $189 \mu\text{g m}^{-3}$ are simulated for Domain 2 with MM5-EMICAT2000-CMAQ when performed nested simulations for 14 August, 2000, at 1200UTC (Figure 4.3)

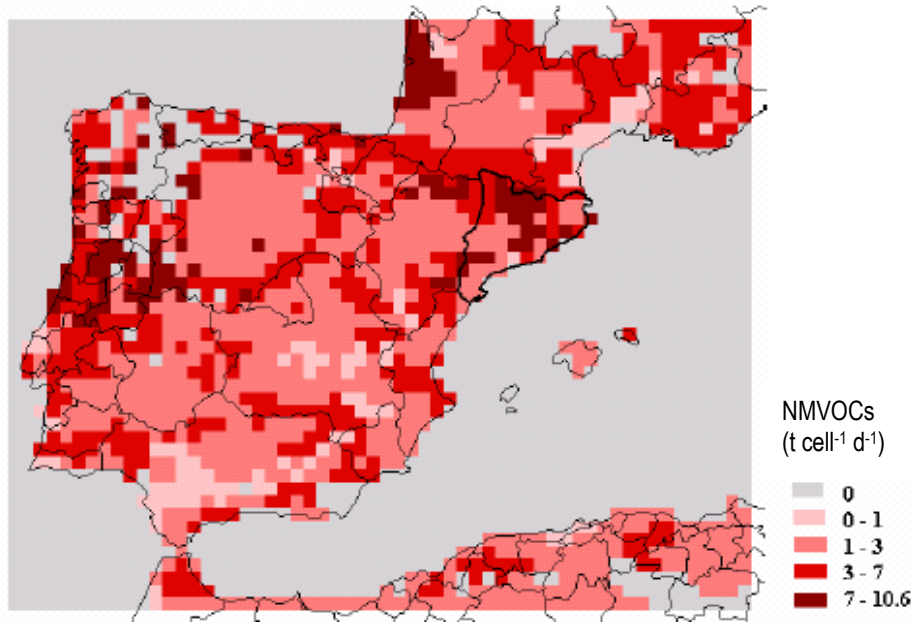


Figure 4.1. Map of biogenic emissions on 15 August, 2000, for the domain 1 (Iberian Peninsula, northern Africa and southern France).

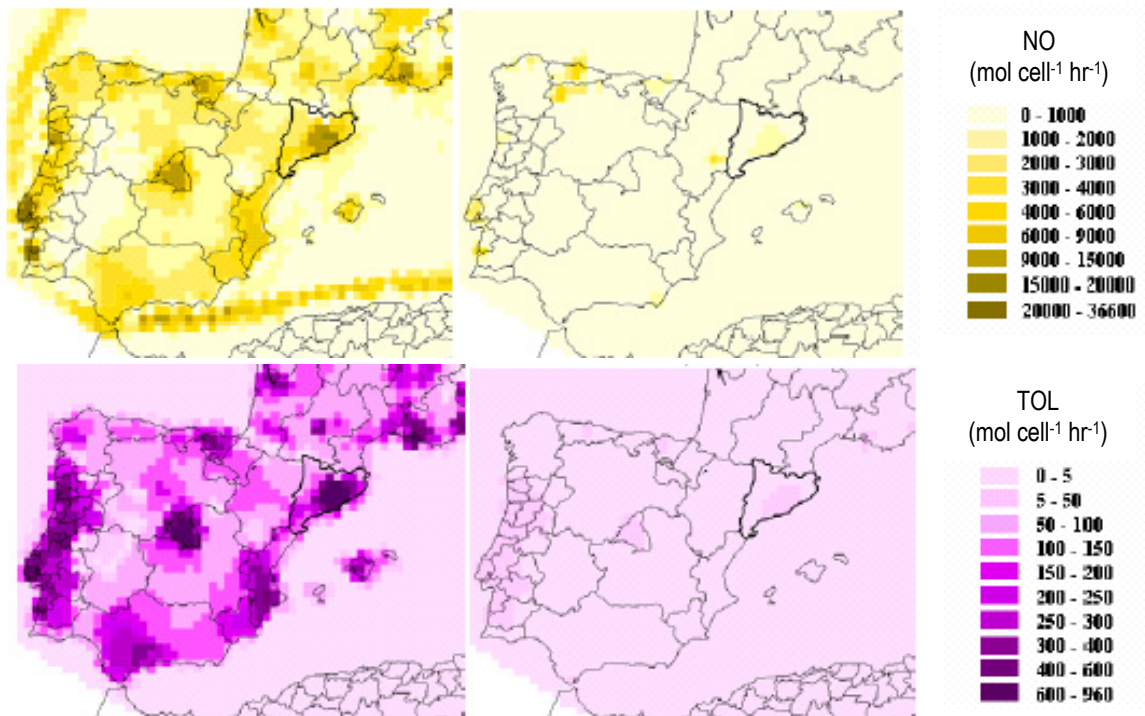


Figure 4.2. Map of emissions on 13 August, 2000, at 1200UTC for the domain 1 (Iberian Peninsula, northern Africa and southern France) for categories NO and TOL of CBM-IV mechanism: (left) surface; and (right) 150m height.

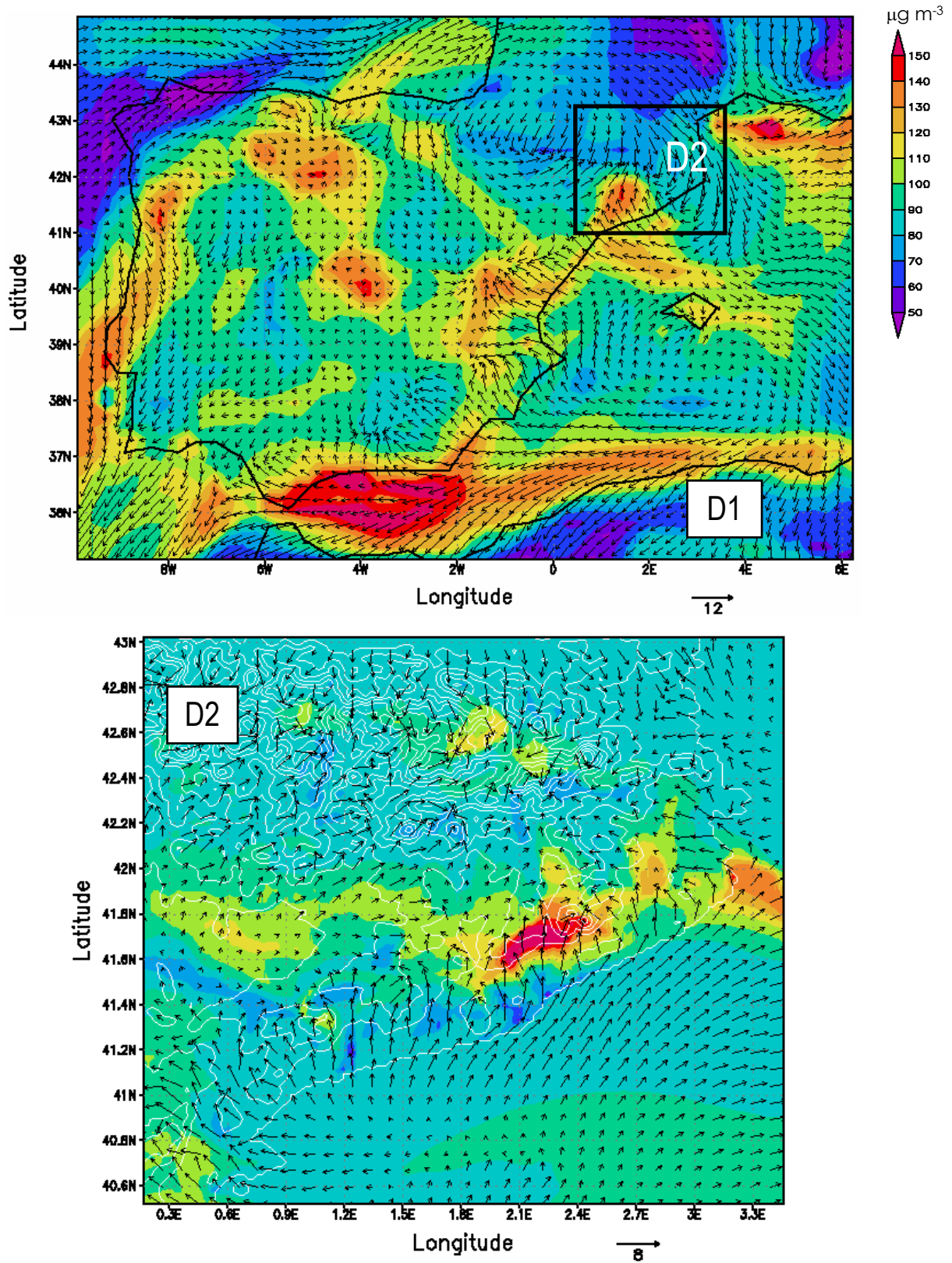


Figure 4.3. Ozone concentrations ($\mu\text{g m}^{-3}$) and wind field vectors for Domain 1 (Iberian Peninsula) and Domain 2 (northeastern Iberian Peninsula) at 1200UTC on 14 August, 2000.

The evolution of the flows and the concentrations of photochemical pollutants for a daily cycle over the Iberian Peninsula (D1) are shown in Figures 4.4, 4.5 and 4.6 in the cases of ozone, carbon monoxide and nitrogen oxides, respectively. Simulations depict the results for 14 August, 2000, in the Domain 1 (covering the Iberian Peninsula, northern Africa and southern France) since this day is representative of the episode of pollution covering 13-16 August, 2000, characterized by thermal circulations that dominate most of the Peninsula for these four days.

The nocturnal regime is characterized by the development of mountain and katabatic winds in the main orographic systems and the formation of land breezes in coastal areas. In the west littoral, flows are influenced by the anticyclonic dorsal. At night, there are three important drainages of pollutants in D1. First, the drainage through the Ebro Valley in the northeastern part of the Peninsula is hampered by the penetration of hot air masses from the Mediterranean induced by the anticyclonic circulation over the sea (Jorba *et al.*, 2003). Second, flows are canalized between the Pyrenees and the Central Massif, introducing northwestern flows into the Mediterranean through the Gulf of Lyon. This canalization plays an important role, because it is the only pass bringing fresh air into the Western Mediterranean Basin (Gangoiti *et al.*, 2001). Last, polluted air masses are drained in the Guadalquivir Valley, in the southwestern Iberian Peninsula, towards the Gulf of Cádiz.

The diurnal regime is observable from 0800UTC, with the establishment of sea breezes on the coast; and valley and anabatic winds in orographic systems. At 1000UTC, the breeze has a component S-SE in the northeastern littoral of the Iberian Peninsula, E in the southern coast and NW-N in the northern coast. The sea flows penetrate through orographic canalizations, reinforced with thermal diurnal circulations and the anabatic winds in the coastal mountain ranges.

Millán *et al.* (1992) define the behavior of breezes in the Western Mediterranean Coast as a coalescence of the breeze circulation with other thermal circulations, originating a *macro-breeze* when the breeze cell joins the convective cell developed in the central plateaus. Jorba *et al.* (2003) describe these processes in the eastern coast of the Iberian Peninsula using numerical weather prediction models.

The surface heating during daytime hours and the convergence of flows inland the Iberian Peninsula produces the development of the Iberian Thermal Low (Millán *et al.*, 1992; 1996; 1997), which leads to very weak circulations in the central Plateau. The maximum development of the Iberian Thermal Low is observed around 1800UTC. The pressure gradient in the central Plateau of the Iberian Peninsula is negligible. From 2000UTC, flows weaken and the nocturnal regimen dominates the dynamics of air pollutants. Drainages are developed in main valleys and peninsular orographic systems.

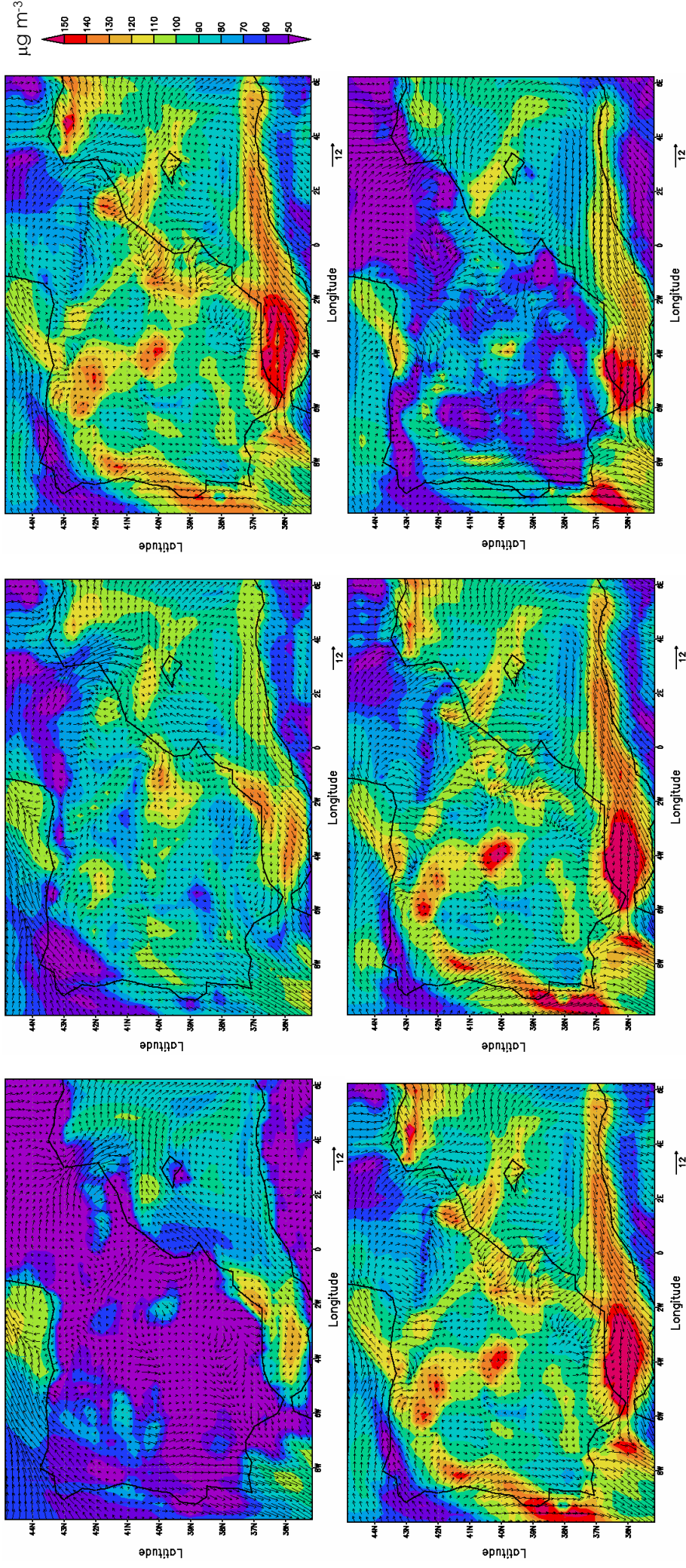


Figure 4.4. Ozone concentrations ($\mu\text{g m}^{-3}$) and wind field vectors at ground level over the Domain 1 (Iberian Peninsula) with MM5-EMICAT2000-CMAQ on 14 August, 2000, at (from up-left to down-right) 0600 UTC, 1000UTC, 1200UTC, 1400UTC, 1600UTC and 2000UTC.

Air quality modeling in very complex terrains: ozone dynamics in the northeastern Iberian Peninsula

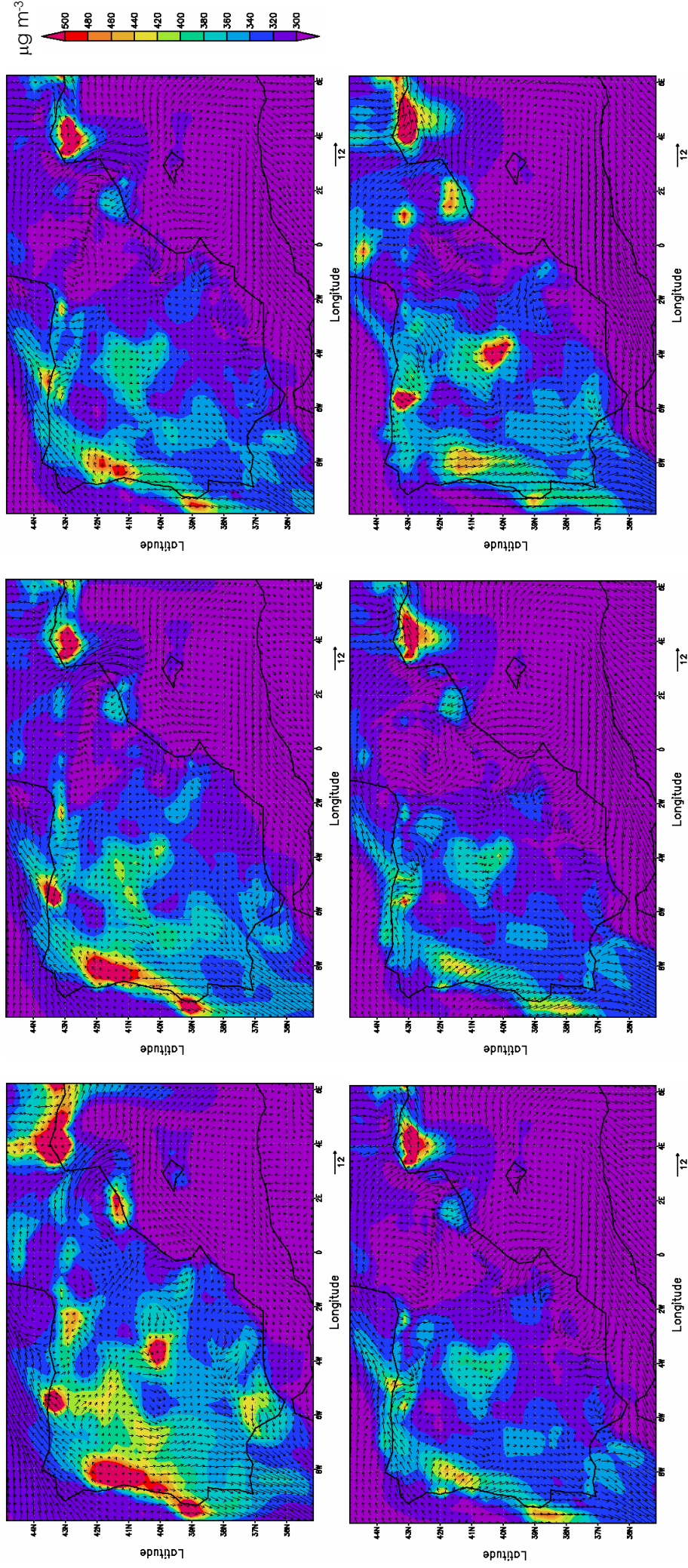


Figure 4.5. Carbon monoxide concentrations ($\mu\text{g m}^{-3}$) and wind field vectors at ground level over the Domain 1 (Iberian Peninsula) with MM5-EMICAT2000-CMAQ on 14 August, 2000, at (from up-left to down-right) 0600 UTC, 1000UTC, 1400UTC, 1600UTC and 2000UTC.

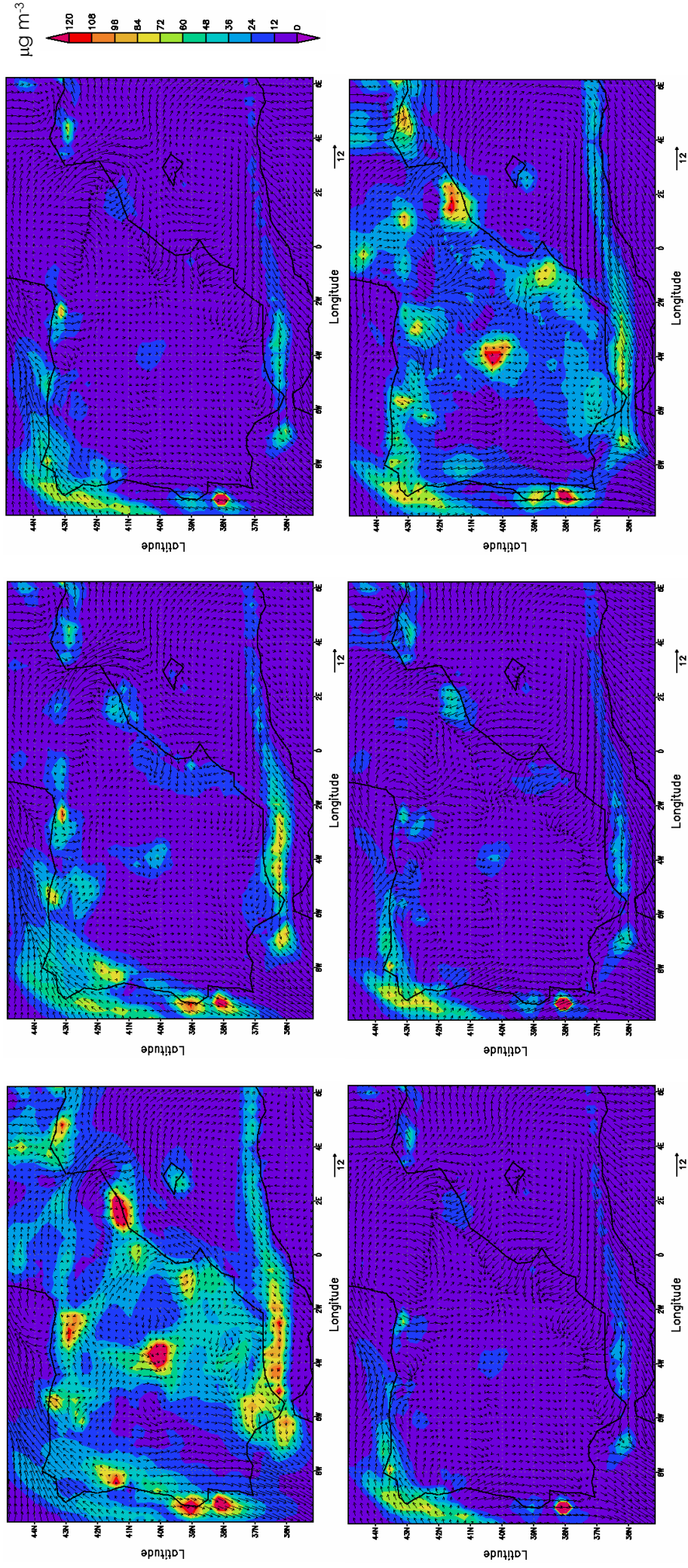


Figure 4.6. Nitrogen oxides concentrations ($\mu\text{g m}^{-3}$) and wind field vectors at ground level over the Domain 1 (Iberian Peninsula) with MM5-EMICAT2000-CMAQ on 14 August, 2000, at (from up-left to down-right) 0600 UTC, 1000UTC, 1200UTC, 1400UTC, 1600UTC and 2000UTC.

In order to assess the influence of initial and boundary conditions in tropospheric ozone levels, different simulations were performed in D2 by modifying the initial and boundary conditions generated from the nested simulation of D1. Apart from the base case, five different scenarios were defined: (1) Scenario 1: increase of +50% in ozone initial conditions; (2) Scenario 2: +50% in ozone precursors' initial conditions; (3) Scenario 3: increase of +50% in ozone boundary conditions; (4) Scenario 4: +50% in ozone precursors' boundary conditions; and (5) Scenario 5: clean boundary conditions.

4.3.1 Influence of Initial and Boundary Conditions

The entire domain of the northeastern Iberian Peninsula is analyzed; however, four sites are selected to highlight the sensitivities to initial and boundary conditions (Figure 4.7), attending to their proximity to the different boundaries, their different sensitivity to NO_x and VOCs emissions (Jiménez and Baldasano, 2004) and their characteristics. Therefore, sites 1 (Sort) and 4 (la Sénia) are background scenarios where the influence of initial and boundary conditions is higher than in urban locations (site 2, Vic, and site 3, Barcelona), where the local emissions-photochemistry cycle may play a more important role. For these scenarios and sites, the basic features of the evolution of ozone and the affected response by modifying the initial and boundary conditions in MM5-EMICAT2000-CMAQ is represented.

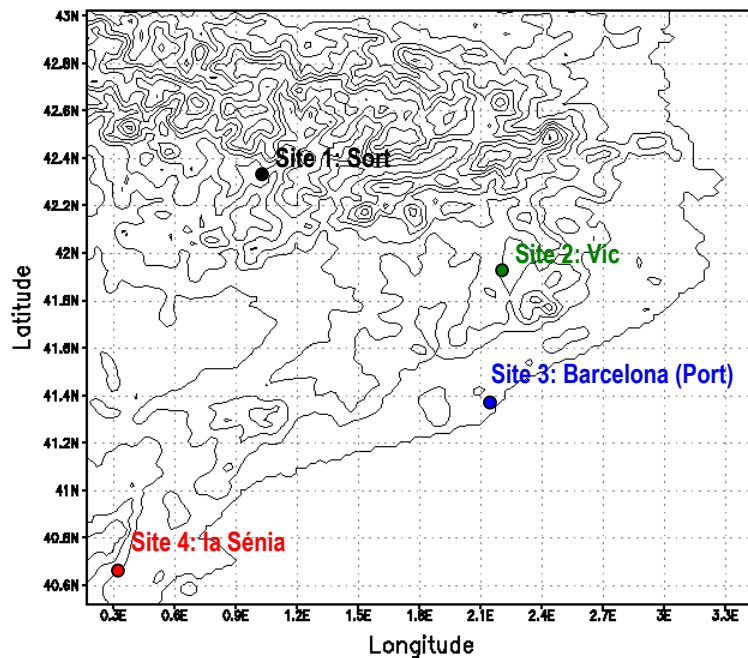


Figure 4.7. Location of sites within the domain of the northeastern Iberian Peninsula (D2) included in the analysis of the influence of initial and boundary conditions.

In Figure 4.8, the arrival time of boundary conditions varied with the selected sites depending on their distance to the upwind boundary condition. The arrival times of boundary conditions were 22, 36, 24 and 1-hr for sites 1-4, respectively. For a same species, longer arrival time of boundary conditions allows more time for simulated tracers to decay further during the transport processes and results in a weaker influence of boundary conditions (Liu *et al.*, 2001).

The impacts of both initial and boundary conditions on ozone concentrations may fluctuate with time during the simulation period (Figure 4.8). The fluctuations are caused by the different behavior of emissions and wind fields during the episode selected. The percentual difference between Scenario 1 (+50% ozone in initial conditions) and the base case shows a secondary maximum in urban sites (Site 2: Vic and Site 3: Barcelona) after 30 hours of the beginning of the simulation, with deviations exceeding the 50%. After this maximum, a sudden decrease is produced, being the impact factor fewer than 10% after approximately 40 hours. A possible explanation of these fluctuations is found in Liu *et al.* (2001), where it is indicated that different heights of mixing layer between day and night also lead to fluctuated differences between diverse scenarios.

The impact factor for increasing the initial or boundary concentrations of precursors (Scenarios 2 and 4, respectively) remains under 15% for all the period of simulation, and is negligible after 36 hours of spin-up time. It should be highlighted that, for Site 4 (la Sènia), Scenario 4 leads to slightly higher decreases of O₃ concentrations at night respect to the base case, because of a higher O₃ depletion throughout the reaction with NO introduced by boundary conditions. On the other side, this increase in precursors makes ozone concentrations exceed the levels of the base case on a 15-20% during the hours of daylight. However, this pattern is not observed in other sites further from boundaries. Ozone in Scenario 4 increases rapidly after 36 hours of simulation to a 10% difference respect to the base case and progressively reaches a 20% difference 72 hours after the start of the studio. Because of the lack of anthropogenic emissions in background areas, the proximity of la Sènia to the south and western boundary makes the difference between the Scenario 3 (+50% ozone in boundaries) and the base case reach 50% after just 4 hours of the start. This impact factor remains practically constant during the simulation period; therefore, the transport of external pollutants through the boundaries dominates the levels of O₃ in this location, as will be discussed later in Section 4.3.2 for simulations with clean boundaries.

In comparison with the influence of boundary conditions, the impact of initial condition decays approximately in an exponential way and presents an anti-correlated behavior respect to the boundary conditions. Focusing on processes within the boundary layer, a 48 hour spin-up time is sufficient to reduce the impact factor of initial conditions to 0.1 or less for ozone in all sites, both when incrementing ozone or precursors in the boundary concentrations. On the other side, the impact factor is controlled by the boundary conditions after a certain time of simulation, related to the arrival of upwind air masses. This impact factor for boundary conditions stabilizes around 50% after 48 hours for Sites 1, 3 and 4, and fluctuates in the simulations for Site 2, achieving a factor of 70% after 72 hours of the beginning of simulations.

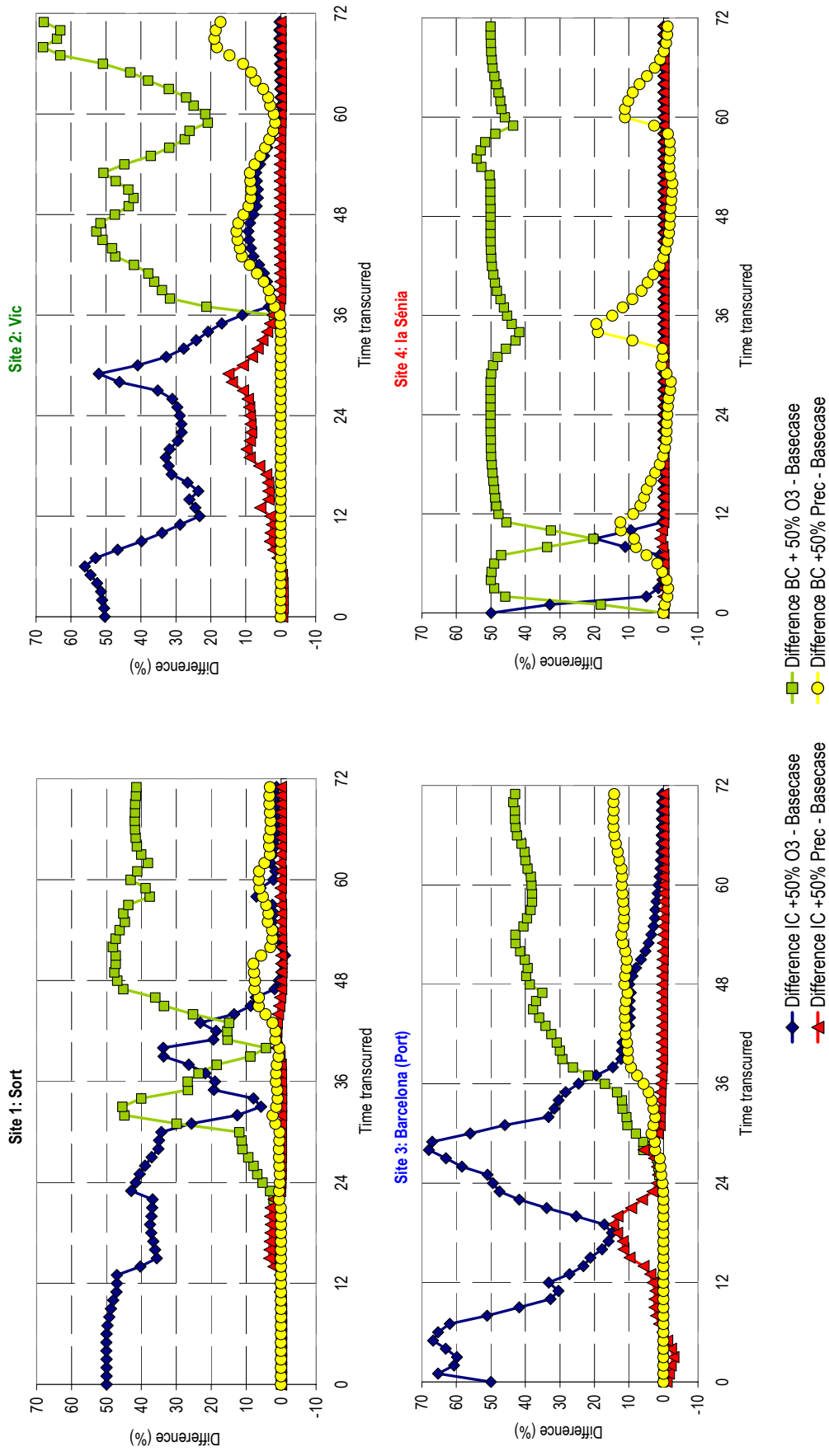


Figure 4.8. Difference in ozone concentration (%): evolution of the different scenarios for the sites defined in Figure 4.7: Sort, Vic, Barcelona-Port and la Sénia.

It is also noteworthy that the influence of initial conditions can still remain significant when the air parcel from the boundary arrives. Therefore, the start-up or spin-up helps reducing the influence of initial conditions, but it also introduces the influence of boundary condition in the case of ozone. For other species with longer lifetime, Berge *et al.* (2001) report that this fact is especially true for the upper troposphere, since lifetimes of chemical species there are usually longer.

Impacts of initial conditions on the estimated results by MM5-EMICAT2000-CMAQ for the entire domain of the northeastern Iberian Peninsula are illustrated in Figure 4.9 for Scenario 1 (+50% ozone in initial conditions) and Figure 4.10 for Scenario 2 (+50% precursors in initial conditions). In the case of Scenario 1 (Figure 4.9), differences in ozone concentrations at the beginning of the simulation are specially important over the areas with higher O_3 levels at night, that are mainly rural areas (Pyrenees, St. Llorenç, etc.) and the Mediterranean Sea. After 24 hours of simulations, differences are minimized over the northern, western and southern parts of the domains, where ozone concentrations are conditioned by the ozone transport through the boundaries, which remain equal for Scenario 1 and base case.

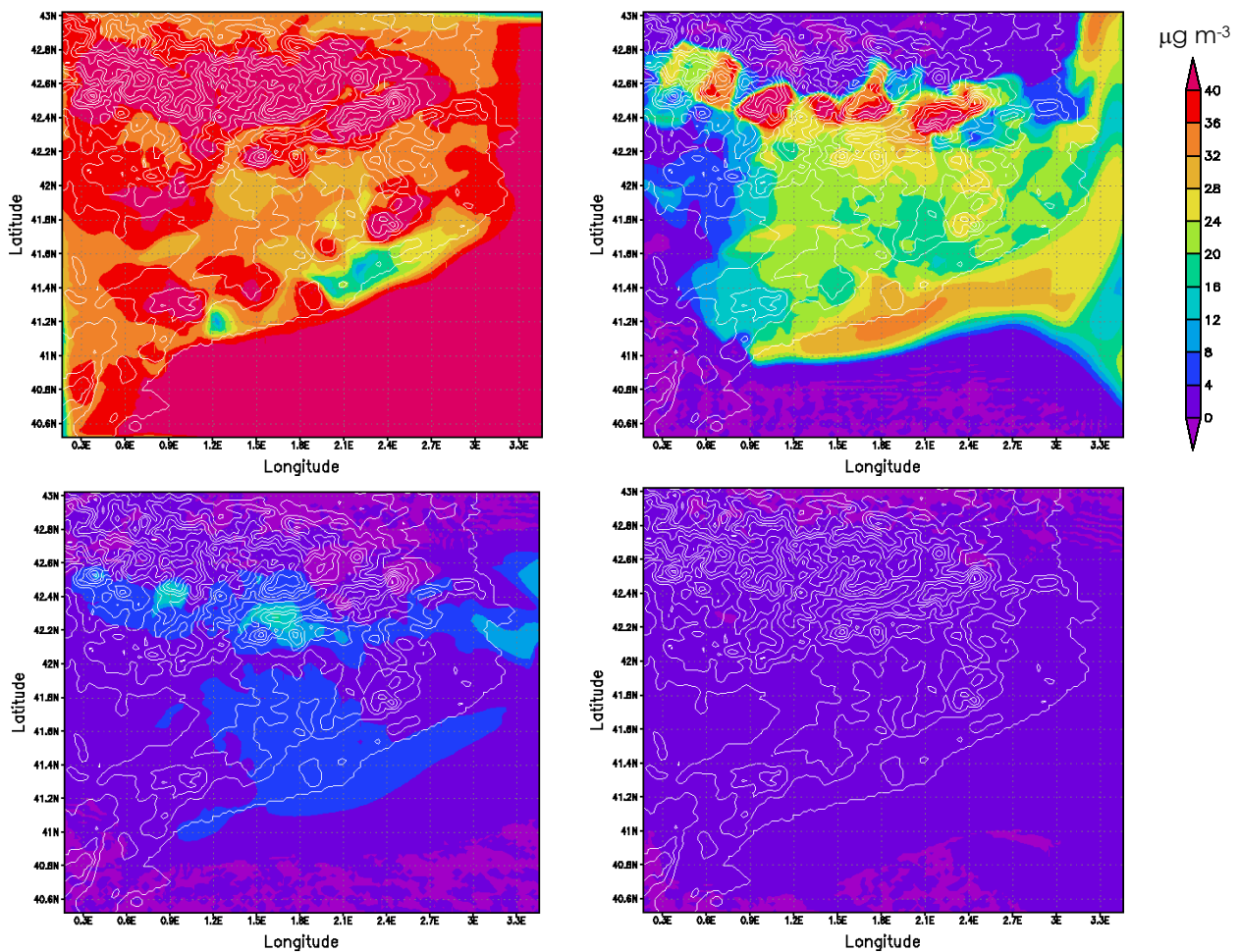


Figure 4.9. Difference Scenario 1 (+50% in ozone initial conditions) – base case after (from up-down and left-right) 0, 24, 48 and 72 hours of the beginning of simulation.

At this time, the impact of initial conditions is important over the Pyrenees and the tongue-shaped area covering coastal sites, where the emissions-photochemistry cycle plays an important role and gets more affected because of the initial concentrations. The influence in O_3 levels may achieve $30 \mu\text{g m}^{-3}$ in the littoral of the northeastern Iberian Peninsula (Figure 4.9). Inland, these variations are in the order of $20\text{-}25 \mu\text{g m}^{-3}$. However, after 48 hours of the beginning, the differences between Scenario 1 and the base case have reduced to approximately $15 \mu\text{g m}^{-3}$ in the sub-Pyrenees and $5 \mu\text{g m}^{-3}$ in coastal sites. The rest of the domain presents no variances respect to the base case that are negligible when a spin-up time of 72 hours is considered.

The differences between the Scenario 2 and the base case (Figure 4.10) are negligible for ozone concentrations at the beginning of the simulation. Afterwards, main differences are observed in the photochemically aged masses departing from the city of Barcelona, where an increase in the concentrations of precursors at the start of simulations lead to a higher formation of ozone during the hours of photochemical activity. However, these air masses with a higher concentration of ozone and precursors respect to the base case are transported by mesoscale flows during the development of the sea-land breezes cycles, extracting them from the area of study (as observed in the area over the northeastern limit of the domain after 24 hours of simulation).

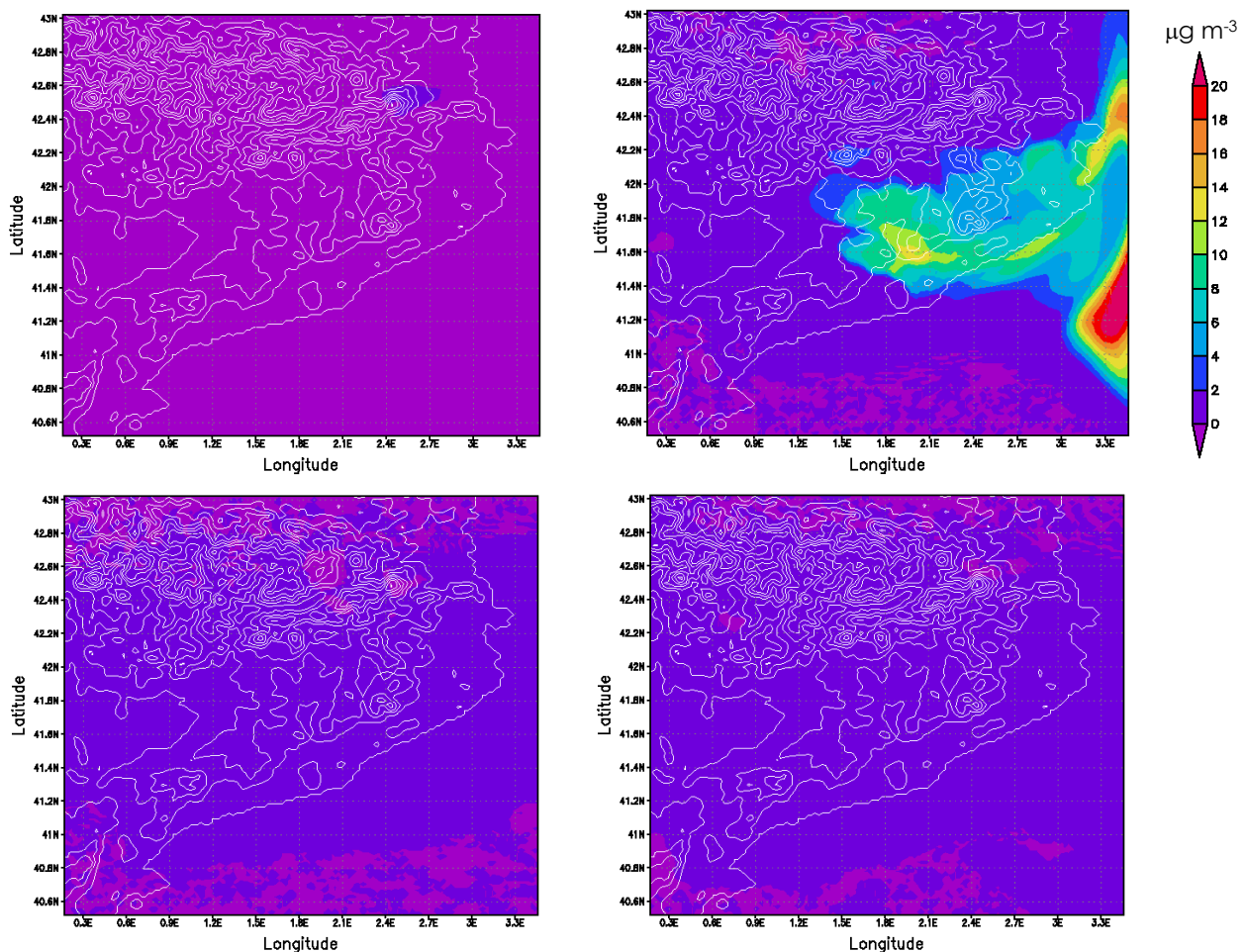


Figure 4.10. Difference of Scenario 2 (+50% in initial conditions of precursors) – base case (from up-down and left-right) after 0, 24, 48 and 72 hours of the beginning of simulation.

Once this ozone-rich air mass, as a consequence of +50% of precursors in initial conditions, has been extracted from the domain, the local emissions (equal for Scenario 2 and base case) dominate the photochemical cycle and the impact is negligible after 48-72 hours of the beginning of the simulation.

Figure 4.11 for Scenario 3 (+50% ozone in boundaries) and Figure 4.12 in the case of Scenario 4 (+50% precursors in boundaries) demonstrate that if the arrival time of the boundary condition is small, then the O_3 concentrations are significantly affected by the value of boundary conditions. When the arrival time of boundary condition is large, influences of initial and boundary conditions are greatly reduced due to the decaying effects, and the estimated O_3 concentrations are mainly contributed by the local and upwind characteristics. The difference of O_3 concentration progressively increases during the simulation. In Scenario 3 (Figure 4.11), after 24 h, minimal differences are observed between Scenario 3 and the base case.

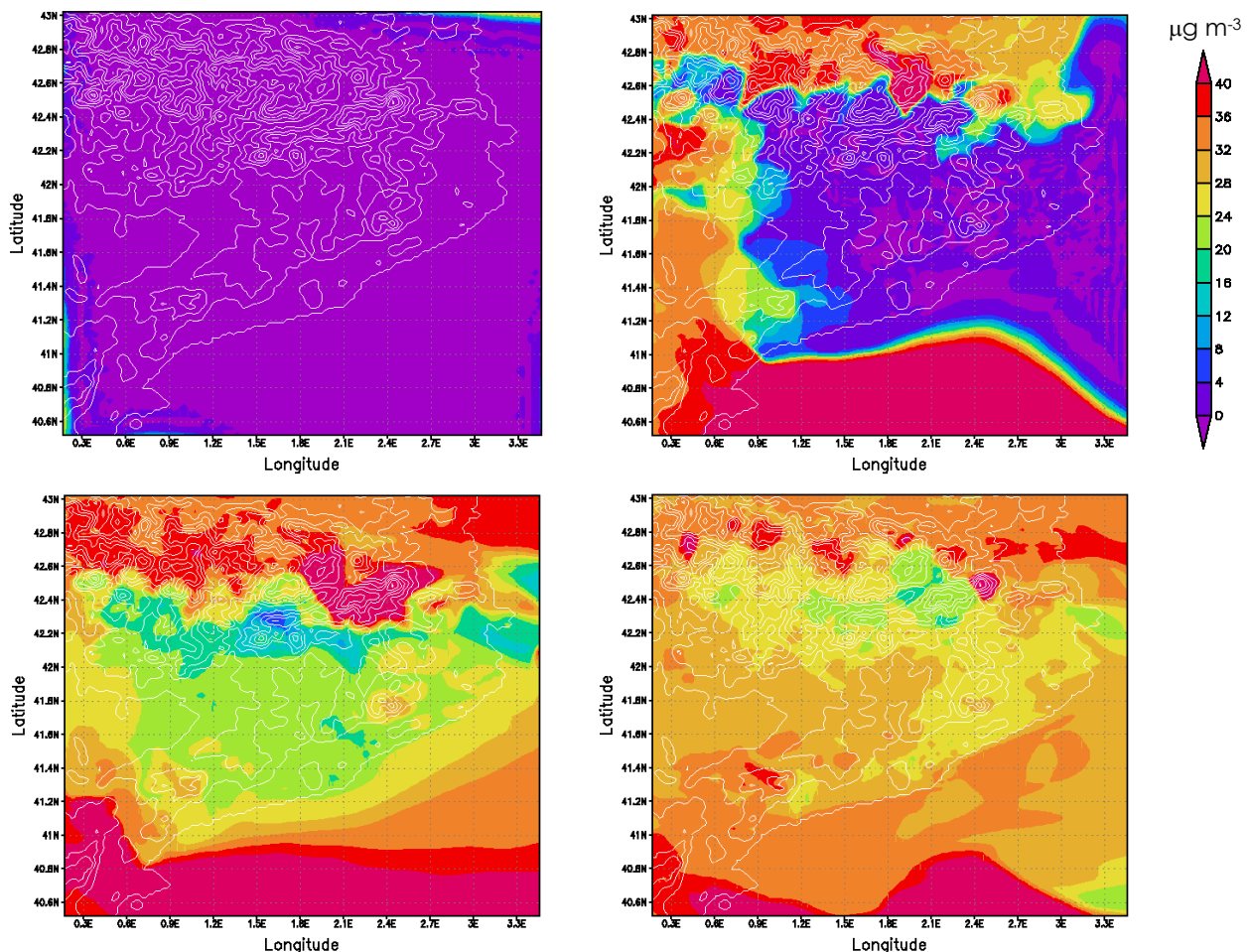


Figure 4.11. Difference Scenario 3 (+50% in ozone boundary conditions) – base case after (from up-down and left-right) 0, 24, 48 and 72 hours of the beginning of simulation.

Concentrations of ozone $40 \mu\text{g m}^{-3}$ higher than those of the base case are found over the Mediterranean Sea in the southern part of the domain and in the Pyrenees in Scenario 3 at that time, that remain practically constant during the 72 hours of simulation. Pollutants (mainly, photochemically aged air masses with high concentrations of ozone and poor in photochemical precursors) are transported to the Mediterranean area, where they sink within the anticyclone located over the Western Mediterranean Sea (Gangoiti *et al.*, 2001). A fraction of these pollutants are advected out from the domain of the northeastern Iberian Peninsula, and the other fraction is incorporated on the following morning to the sea-breeze cycle.

This transport through the southern boundary indicates a reservoir layer of ozone that remains over the Mediterranean Sea during the episode of 13-16 of August, 2000 (which may be observed in Figure 4.4). The development of sea breezes cycles re-circulates these air masses again into the domain of the northeastern Iberian Peninsula. This agrees with the results by Millán *et al.*, (1996; 1997), Toll and Baldasano (2000) and Pérez *et al.* (2004). All these processes will be analyzed in detail in Chapter 6.

Furthermore, the transport of pollutants with a peninsular origin through the western boundary may have a certain importance in sites near this boundary ($25 \mu\text{g m}^{-3}$ after 48 hours and around $35 \mu\text{g m}^{-3}$ in the western boundary). Last, in the middle of the domain, boundaries arrive after approximately 20-30 hours after the beginning of the simulation, depending on the site, and differences of Scenario 3 respect to the base case reach $30 \mu\text{g m}^{-3}$ inland the northeastern Iberian Peninsula after 72 hours.

For Scenario 4 (Figure 4.12), the main transport of precursors appears to be produced through the western boundary (Peninsular origin). That phenomenon causes increments in ozone concentrations around $20 \mu\text{g m}^{-3}$ in Plana de Lleida and $15 \mu\text{g m}^{-3}$ in the Mediterranean sea after 24 hours of simulation. The reservoir layer over the Mediterranean is poor in precursors (as observed in Figures 4.5 and 4.6 for the simulation of precursors of the Domain 1), and therefore southern boundary does not seem to present a relevant influence on ozone concentrations on the following days. After 48 hours, the westerly winds have transported precursors over the littoral mountains, and they influence all the coastal line and the Mediterranean Sea with differences respect to the base case over $15\text{-}20 \mu\text{g m}^{-3}$. Finally, after 72 hours, concentrations in the central plateaus and the southeastern part of domain are controlled by the participation of precursors introduced through the boundaries into the domain.

Both for Scenarios 3 and 4, it may be summarized that if the concentrations of both ozone and its precursors in the boundary conditions are overestimated by 50%, after the downwind transport, influences of this error remain during the entire period of simulation especially in those background areas where the influence of advective transport through the boundaries is relevant.

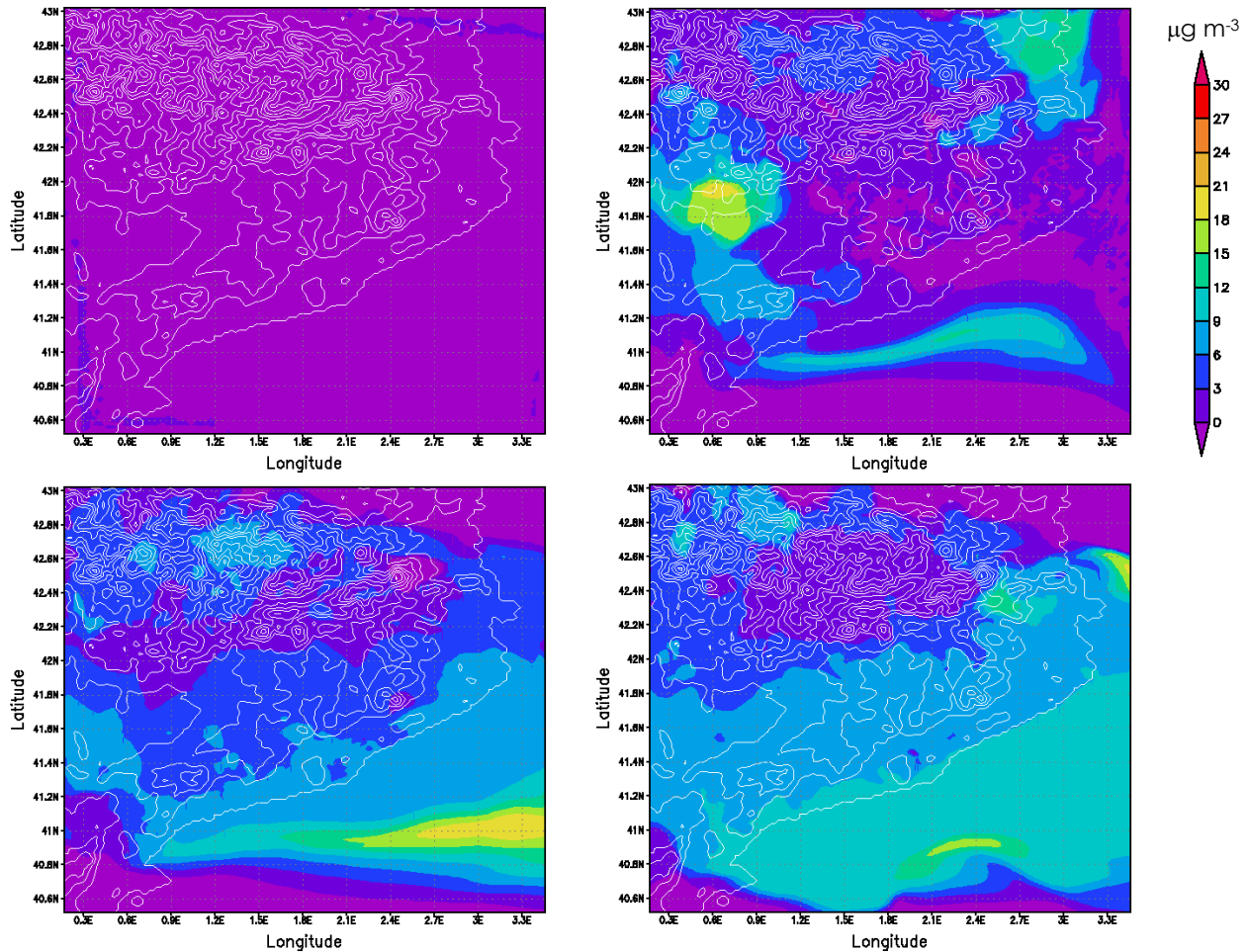


Figure 4.12. Difference Scenario 4 (+50% in boundary conditions of precursors) – base case after (from up-down and left-right) 0, 24, 48 and 72 hours of the beginning of simulation.

4.3.2 Analysis of Advective Transport by Using Clean Boundary Conditions

In order to account for the advective transport through the boundary conditions to ozone levels, simulations with MM5-EMICAT2000-CMAQ for the domain of the northeastern Iberian Peninsula were conducted with clean boundary conditions respect to the base case simulations. These results within the boundary layer are shown in Figure 4.13 for 1-hr maximum ozone levels and Figure 4.14 for daily average ozone levels.

The modeled ozone with MM5-EMICAT2000-CMAQ indicates that the most important influence of advective transport on ozone (both for 1-hr maximum concentrations and average levels) is produced over the Mediterranean Sea. Maximum simulated 1-hr ozone concentration is achieved downwind the city of Barcelona, in latitude 41.842 N and longitude 2.305 E ($189.1 \mu\text{g m}^{-3}$ in the base case, and $184.4 \mu\text{g m}^{-3}$ in the case with clean boundary conditions). Therefore, the contribution of advective transport to maximum ozone levels is $4.7 \mu\text{g m}^{-3}$, which signifies a 2.5% of the final maximum concentrations.

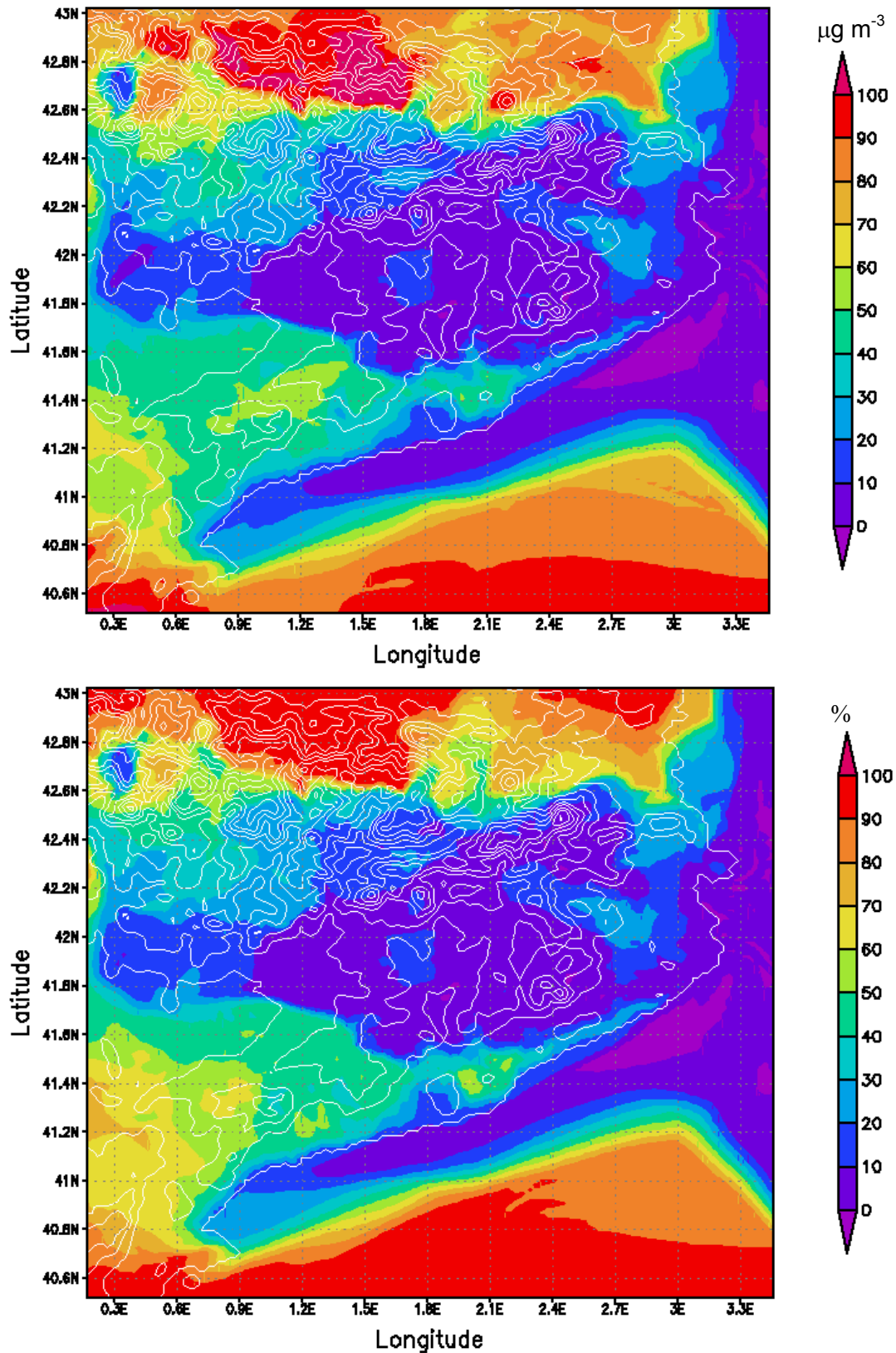


Figure 4.13. Difference in the ozone results of the base simulation minus simulation with clean boundaries in the PBL of the northeastern Iberian Peninsula for 13-16 August, 2000: (up) difference in maximum 1-hr concentrations ($\mu\text{g m}^{-3}$) and (down) percentual difference for 1-hr peak respect to the base simulation.

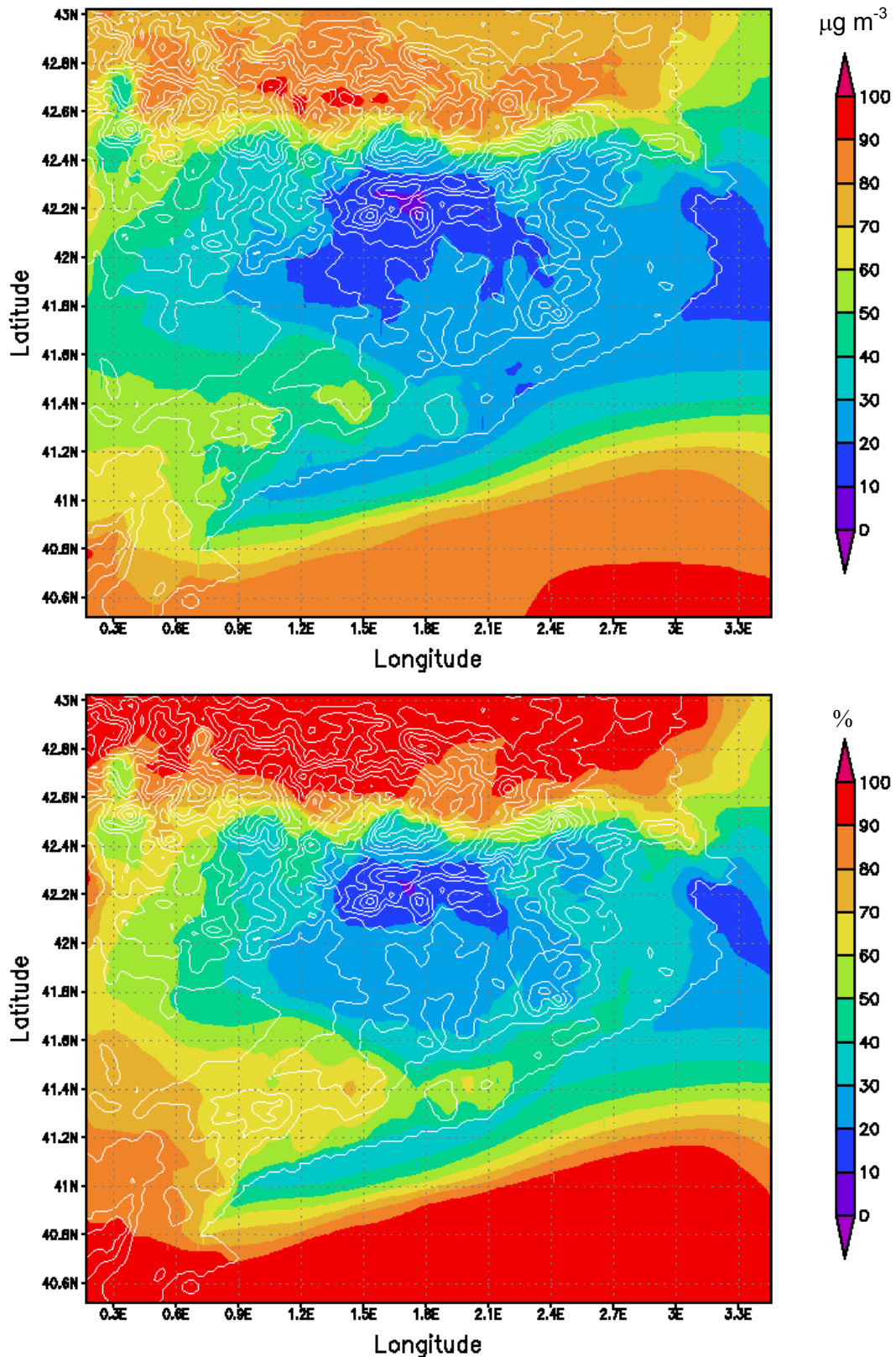


Figure 4.14. Difference in the ozone results of the base simulation minus simulation with clean boundaries in the PBL of the northeastern Iberian Peninsula for 13-16 August, 2000: (up) difference in daily average concentrations ($\mu\text{g m}^{-3}$) and (down) percentual difference for mean concentrations respect to the base simulation.

As shown in Figure 4.4 there is an important reservoir of ozone over the Western Mediterranean coast and the Balearic Islands, which is transported again to the domain through the southern boundary with the development of the sea breeze. This O_3 accounts for $90 \mu\text{g m}^{-3}$; however, the dominant chemistry in the Levantine coast of the northeastern Iberian Peninsula is dominated by local photochemistry. In coastal areas, the strong forcing of emissions is the most relevant process, having the advective transport an importance of 5%-10% (around $10 \mu\text{g m}^{-3}$) respect to maximum ozone levels in these areas. The contribution to daily average levels is more important, around 30% in these areas ($20 \mu\text{g m}^{-3}$) since of the vertical descend of ozone reservoir layers during the night as a consequence of the compensatory subsidence (Pérez *et al.*, 2004), which introduces ozone in the lower troposphere and the planetary boundary layer.

In addition, the transport through the western boundary (air with an origin set in the Iberian Peninsula) may help to the 1-hr peak levels achieved in the plain of Lleida with $50 \mu\text{g m}^{-3}$. In this area, due to the lack of anthropogenic emissions, the advective transport represents over 70% of the ozone within the planetary boundary layer, highly contributing to background levels. With respect to average daily levels, the advective transport of air masses through the western boundary is the responsible for nearly the 90% of the O_3 in the western domain of study, contributing with $60\text{-}70 \mu\text{g m}^{-3}$ to the ozone produced photochemically in the area. The origin of these air masses, as will be detailed in Chapter 6, may be explained by the peninsular transport of polluted air masses and the polluted air masses from the industrial area of Castellón that, due to the anticyclonic circulations, enter in the northeastern Iberian Peninsula throughout the south and western boundaries. The influence of the northern boundary condition on ozone concentrations in the northern slope of the Pyrenees (air masses with a background origin from Atlantic ocean and southern France) is also important. Here, the transport of ozone from outside the northeastern Iberian Peninsula domain could account for over 90% of both average and 1-hr peak concentrations.

4.4 Conclusions

Although initial and boundary condition specifications are recognized as an important issue in air quality modeling, systematic studies of their impacts are scarce. In this work, a description of the process of initialization and generation of boundary conditions for MM5-EMICAT2000-CMAQ through performing simulations in the entire Iberian Peninsula, and using a multiscale approach in order to provide the necessary boundaries for a domain in the northeastern Iberian Peninsula. Furthermore, analyses of the influences of initial and boundary conditions and their sensitivity on ozone results are presented, indicating the necessity of a correct initialization of the model by means of spin-up or start-up procedures; and also the availability of good-quality boundary information when performing simulations in very complex terrains.

Results suggest that the impacts of initial conditions on a given site decrease with simulation time and significantly affect the species concentrations before the arrival of boundary conditions, and are negligible after their arrival. Therefore, the influence of initial conditions could be minimized through spin-up or start-up prior to formal simulations. Focusing on the conditions within the planetary boundary layer, a 48-hour spin-up time is sufficient to reduce the impact factor of initial conditions to 10% or less for ozone. Because of the model is initialized at 0000UTC, the influence of the modification of ozone precursors on initial conditions is very low during the nighttime hours, increases until 30-hr after the begin of the simulations and then decreases dramatically since the influence of pervasive local emissions that are much higher than the remaining contribution of initial precursors.

The influence of boundary conditions is significant to a selected site when the arrival time of boundary condition is short and the species lifetime is longer, as the case of ozone. The impact of modifying boundary precursors in ground-level ozone keeps under 20% during the whole period of simulations for most sites in the northeastern Iberian Peninsula, since boundaries of the domain selected are far enough from relevant sites not to have a significant influence. The effect of modifying ozone boundaries becomes evident after 30-hr, when the impact factor of boundary conditions overcomes the value of 10% for ground-level ozone, and dominates over the effect of initial conditions after 35 hours of the beginning of the simulation. Results indicate that influences of boundary conditions are more important for areas near domain boundaries, especially in background areas where contribution of ozone precursors is due to a short-medium range transport.

In order to account for the advective transport through the boundary conditions to ozone levels, simulations were conducted with clean boundary conditions respect to the base case simulations. The modeled ozone indicates that the most important influence of advective transport on ozone is produced over the Mediterranean Sea. However, the particular conditions of the episode simulated (low pressure gradient meteorological conditions, with limitations in the advective transport and a strong dominance of the local emissions-photochemistry cycle) makes that the contribution of advective transport to maximum ozone levels is just $4.7 \mu\text{g m}^{-3}$, which signifies just a 2.5% of the final maximum concentrations.

Finally, it should be highlighted that, despite the influence of initial conditions may be minimized through a proper spin-up time of 48 hours (this spin-up time will be used in subsequent simulations with MM5-EMICAT2000-CMAQ for different studies presented in this Dissertation), the importance of boundary conditions becomes essential and their contribution in ozone concentrations over the domain increase with the time of simulation. Therefore, it is necessary to carefully consider this issue when applying air quality models. In this work, this problem is resolved by including all the sources that have potential effects on the given region in the domain of the northeastern Iberian Peninsula; and by applying the nested simulation results of a larger

model domain covering the entire Iberian Peninsula to the boundary conditions of smaller nested simulation domain.

4.5 References

- Byun, D.W., Young, J., Odman, M.T., 1999. Governing equations and computational structure of the Community Multiscale Air Quality (CMAQ) chemical transport model. In: Byun, D.W., Ching, J.K.S. (Eds.), Science algorithms of the EPA Models-3 Community Multiscale Air Quality System (CMAQ) modeling system. Atmospheric Modeling Division, U.S. Environmental Protection Agency, Research Triangle Park, NC, EPA 600/R-99/030.
- Berge, E., Huang, H.-C., Chang, J., Liu, T.-H., 2001. A study of the importance of initial conditions for photochemical oxidant modeling. *Journal of Geophysical Research*, **106**(D1), 1346-1363.
- Gangoiti, G., Millán, M.M., Salvador, R., Mantilla, E., 2001. Long-range transport and re-circulation of pollutants in the western Mediterranean during the project regional cycles of air pollution in the west-central Mediterranean area. *Atmospheric Environment*, **35**, 6267-6276.
- Gery, M.W., Whitten, G.Z., Killus, J.P., Dodge, M.C., 1989. A photochemical kinetics mechanism for urban and regional scale computer modeling. *Journal of Geophysical Research*, **94** (D10), 12925-12956.
- Jiménez, P., Baldasano, J.M., 2004. Ozone response to precursor controls: the use of photochemical indicators to assess O₃-NO_x-VOC sensitivity in the northeastern Iberian Peninsula. *Journal of Geophysical Research*, **109**, D20309, doi: 10.1029/2004JD004985.
- Jorba, O., Gassó, S., Baldasano, J.M., 2003. Regional circulations within the Iberian Peninsula east coast. In: 26th NATO/CCMS International Technical Meeting on Air Pollution Modelling and Its Application. Kluwer Academic/Plenum Publishers, 388-395.
- Liu, T.-H., Jeng, F.-T., Huang, H.-C., Berge, E., Chang, J.S., 2001. Influences of initial and boundary conditions on regional and urban scale Eulerian air quality transport model simulations. *Chemosphere-Global Change Science*, **3**, 175-183.
- Millán, M.M., Artiñano, B., Alonso, L., Castro, M., Fernandez-Patier, R., Goberna, J., 1992. Mesometeorological cycles of air pollution in the Iberian Peninsula. Air Pollution Research Report 44. Commission of the European Communities. Brussels, Belgium. 219 pp.
- Millán, M.M., Salvador, R., Mantilla, E., Artiñano, B., 1996. Meteorology and photochemical air pollution in southern Europe: Experimental results from EC research projects. *Atmospheric Environment*, **30**, 1909-1924.
- Millán, M., Salvador, R., Mantilla, E., Kallos, G., 1997. Photooxidant dynamics in the Mediterranean basin in summer: results from European research projects. *Journal of Geophysical Research*, **102**, 8811-8823.
- National Research Council, 1991. Rethinking the ozone problem in urban and regional air pollution. National Academy Press, Washington, DC.
- Odman, M.T., Mathur, R., Alapaty, K., Srivastava, K.R., McRae, D.S., Yamartino, R.J., 1995. Nested and adaptive grids for multiscale air quality modeling. U.S. EPA Workshop on Next Generation Models Computational Algorithms (NGEMCOM), Bay City, MI, June 1995.
- Parra, R., 2004. Development of the EMICAT2000 model for the estimation of air pollutants emissions from Catalonia and its use in photochemical dispersion modeling (in Spanish). Ph.D. Thesis, Technical University of Catalonia, Spain.

- Parra, R., Gassó, S., Baldasano, J.M., 2004. Estimating the biogenic emissions of non-methane volatile organic compounds from the North western Mediterranean vegetation of Catalonia, Spain. *The Science of the Total Environment*, **329**, 241-259.
- Parra R., Baldasano, J.M., 2004 Modelling the on-road traffic emissions from Catalonia (Spain) for photochemical air pollution research. Weekday – weekend differences. In: 12th International Conference on Air Pollution (AP'2004), Rhodes (Greece).
- Pérez, C., Sicard, M., Jorba, O., Comerón, A., Baldasano, J.M., 2004. Summertime re-circulations of air pollutants over the north-eastern Iberian coast observed from systematic EARLINET lidar measurements in Barcelona. *Atmospheric Environment*, **38**, 3983-4000.
- Pineda N., Jorba, O., Jorge, J., Baldasano, J.M., 2004. Using NDVI SPOT-VGT Data to update Land-use Map: Application to a Mesoscale Meteorological Model. *International Journal in Remote Sensing* , **25**(1), 129-143.
- Russell, A., Dennis, R., 2000. NARSTO critical review of photochemical models and modeling. *Atmospheric Environment*, **34**, 2283-2324.
- Seinfeld, J.H., Pandis, S.N., 1998. *Atmospheric chemistry and physics: from air pollution to climate change*. Ed. Wiley-Interscience, New York, 1326 pp.
- Soriano, C., Jorba, O., Baldasano, J.M., 2002. One-way nesting versus two-way nesting: does it really make a difference? In: C. Borrego and G. Suyches, *Air Pollution Modeling and its Application XV*, Kluwer Academic/Plenum Publishers, 177-185 pp.
- Stein, A., 2003. Internal communication
- Toll, I., Baldasano, J.M., 2000. Modeling of photochemical air pollution in the Barcelona area with highly disaggregated anthropogenic and biogenic emissions. *Atmospheric Environment*, **34**, 19, 3060-3084.
- US EPA, 2003. Air Chief 10, Emission Factor and Inventoy Group. US Environmental Protection Agency. Research Triangle Park, NC 27 711 (CD-ROM).